

Validity of linear measurements of the jaws using ultralow-dose MDCT and the iterative techniques of ASIR and MBIR

Asma'a A. Al-Ekrish¹ · Reema Al-Shawaf¹ · Peter Schullian² ·
Ra'ed Al-Sadhan¹ · Romed Hörmann³ · Gerlig Widmann²

Received: 3 February 2016 / Accepted: 5 May 2016 / Published online: 2 June 2016
© CARS 2016

Abstract

Purpose To assess the comparability of linear measurements of dental implant sites recorded from multidetector computed tomography (MDCT) images obtained using standard-dose filtered backprojection (FBP) technique with those from various ultralow doses combined with FBP, adaptive statistical iterative reconstruction (ASIR), and

model-based iterative reconstruction (MBIR) techniques. The results of the study may contribute to MDCT dose optimization for dental implant site imaging.

Methods MDCT scans of two cadavers were acquired using a standard reference protocol and four ultralow-dose test protocols (TP). The volume CT dose index of the different dose protocols ranged from a maximum of 30.48–36.71 mGy to a minimum of 0.44–0.53 mGy. All scans were reconstructed using FBP, ASIR-50, ASIR-100, and MBIR, and either a bone or standard reconstruction kernel. Linear measurements were recorded from standardized images of the jaws by two examiners. Intra- and inter-examiner reliability of the measurements were analyzed using Cronbach's alpha and inter-item correlation. Agreement between the measurements obtained with the reference-dose/FBP protocol and each of the test protocols was determined with Bland–Altman plots and linear regression. Statistical significance was set at a P-value of 0.05.

Results No systematic variation was found between the linear measurements obtained with the reference protocol and the other imaging protocols. The only exceptions were TP3/ASIR-50 (bone kernel) and TP4/ASIR-100 (bone and standard kernels). The mean measurement differences between these three protocols and the reference protocol were within ± 0.1 mm, with the 95 % confidence interval limits being within the range of ± 1.15 mm.

Conclusions A nearly 97.5 % reduction in dose did not significantly affect the height and width measurements of edentulous jaws regardless of the reconstruction algorithm used.

Asma'a A. Al-Ekrish and Gerlig Widmann have contributed equally to this paper.

Electronic supplementary material The online version of this article (doi:10.1007/s11548-016-1419-y) contains supplementary material, which is available to authorized users.

✉ Asma'a A. Al-Ekrish
asma.alekrish@gmail.com; aalekrish@ksu.edu.sa

Reema Al-Shawaf
reema_alshawaf@yahoo.com

Peter Schullian
peter.schullian@i-med.ac.at

Ra'ed Al-Sadhan
rsadhan@ksu.edu.sa

Romed Hörmann
romed.hoermann@i-med.ac.at

Gerlig Widmann
gerlig.widmann@i-med.ac.at

¹ Department of Oral Medicine and Diagnostic Sciences, College of Dentistry, King Saud University, P. O. Box 56810, Riyadh 11564, Kingdom of Saudi Arabia

² Department of Radiology, Medical University of Innsbruck, Innsbruck, Austria

³ Division of Clinical and Functional Anatomy, Medical University of Innsbruck, Innsbruck, Austria

Keywords Algorithms · Dental implants · Image processing · Computer-assisted · Multidetector computed tomography · Radiation dosage · Reproducibility of results

Introduction

The widespread use of multidetector computed tomography (MDCT) in the analysis of prospective dental implant sites, although diagnostically beneficial, may contribute to the increasing collective dose of ionizing radiation to populations [1]. Depending on the imaging protocols used, wide variability exists in the radiation doses imparted by MDCT. Effective dose for a MDCT examination of the jaws has reportedly ranged between 453 and 1410 μSv , depending on the area irradiated and scan protocols [2–4]. Therefore, dose sparing protocols should be used whenever possible, provided the dose reductions do not affect image quality and diagnostic accuracy [5,6]. In addition, low-dose images for dental implant site evaluation and application of computer-assisted surgery must achieve linear measurements with an accuracy at least equal to that of standard MDCT exposure protocols. Linear measurements of ridge dimensions obtained with standard MDCT protocols for dental implant site imaging have demonstrated mean absolute error values (compared to direct bone measurements) of 0.65 mm, with 21 % of the errors being larger than 1 mm [7].

Considerable reductions in radiation dose compared to standard MDCT examinations have been shown to provide adequate contrast resolution for subjective identification of bone margins [4,8–10]. Also, implant site measurements and identification of cortical boundaries of the jaws and the inferior alveolar canal have been shown to be comparable when standard MDCT examinations were compared with such low-dose protocols [8,10,11]. The limiting factor for more aggressive dose reductions in MDCT, however, is the increasing image noise which reduces the contrast-to-noise ratio (CNR). So, further reductions in MDCT doses must be accompanied by measures to reduce image noise.

Potential improvements in image quality with reduced radiation doses may be achieved with the iterative reconstruction techniques (IRTs) of adaptive statistical iterative reconstruction (ASIR) and model-based iterative reconstruction (MBIR) techniques. However, the reduced noise levels produced with IRTs compared to the standard filtered back-projection (FBP) reconstruction may reportedly present as an “oversmoothing” of the image, of which the effect on diagnostic accuracy must be considered [12,13]. Therefore, the IRT used must be carefully considered before its implementation for a particular diagnostic task in order to achieve the optimal balance between acceptable image quality and radiation dose.

The use of IRTs in MDCT imaging of the temporal bone and paranasal sinuses has been shown to have the potential to lower the radiation dose up to 50 % compared with FBP, while maintaining the noise levels seen with FBP [14–16]. Furthermore, the use of ASIR and MBIR reportedly allows significant improvements in subjective image quality

of high-resolution images of the craniofacial bone with 76 and 91 % dose reductions compared with the recommended volume CT dose index (CTDIvol) of sinusitis [17]. Also, compared to a standard cranial emergency imaging protocol, diagnosis of orbital and midfacial fractures was found to be sufficient when ASIR and MBIR were used with dose reductions of 97 and 93 % for dislocated and non-dislocated fractures, respectively [13]. However, to our knowledge, there is no information in the published literature regarding the use of MBIR or ASIR in dental implant site imaging. The use of such techniques has the potential to allow further dose reductions compared to previously reported low-dose MDCT imaging of the jaws. Prior to clinical implementation of such techniques in implant site imaging, however, dose optimization is needed to determine the minimum radiation dose that will yield a diagnostic image [18]. Interpretation of images produced by various combinations of scanning and reconstruction techniques has been advocated as the reference standard for establishing the target image quality and required minimum radiation dose [18].

Therefore, the present study aims to assess the comparability of linear measurements of edentulous ridge dimensions recorded from MDCT images obtained using a standard-dose FBP technique with those from different combinations of ultralow doses and reconstruction techniques (FBP, ASIR, and MBIR). The results of the study may contribute to MDCT dose optimization for dental implant site imaging by demonstrating the lowest dose combination that may yield linear measurements comparable to a reference-dose/FBP protocol.

Materials and methods

Cadaver selection

Complete cadaver heads with edentulous and partially edentulous jaws and with intact soft tissues were selected. The bodies were donated by people who had given their informed consent for their use for scientific and educational purposes prior to death [19,20]. All cadavers were preserved using an arterial injection of an alcohol–glycerin solution and immersion in phenolic acid in water for one to three months [21].

Imaging of the cadavers

The cadaver heads including the mandible were scanned using a 64-multislice CT scanner (Discovery CT750 HD, GE Healthcare, Vienna, Austria). The scan range included the entire skull and mandible. Each cadaver was exposed to a high-resolution reference protocol and 4 low-dose test protocols (LD) (Table 1). All MDCT datasets for both cadavers were acquired with a 0.625 mm slice thickness, and the voxel size was $0.625 \times 0.391 \times 0.391$ mm. There was no movement of the cadavers during and between the five different

Table 1 List of exposure parameters and reconstruction techniques used to produce the various combinations of MDCT image datasets

| Exposure protocol | Reconstruction technique | kV | mAs | Pitch | CTDIvol (mGy) | DLP (mG* cm) | Effective dose (mSv) ^c |
|-------------------------|--------------------------|-----|-----|-------|--------------------|---------------------|-----------------------------------|
| Reference-dose protocol | FBP | 120 | 100 | 0.5 | 36.71 ^a | 931.3 ^a | 4.0 ^a |
| | ASIR-50 | | | | 30.48 ^b | 856.72 ^b | 3.8 ^b |
| | ASIR-100 | | | | | | |
| | MBIR | | | | | | |
| Low-dose protocol 1 | FBP | 100 | 35 | 0.5 | 4.19 ^a | 106.22 ^a | 0.5 ^a |
| | ASIR-50 | | | | 3.48 ^b | 97.84 ^b | 0.4 ^b |
| | ASIR-100 | | | | | | |
| | MBIR | | | | | | |
| Low-dose protocol 2 | FBP | 80 | 40 | 0.5 | 2.64 ^a | 66.91 ^a | 0.3 |
| | ASIR-50 | | | | 2.19 ^b | 61.6 ^b | |
| | ASIR-100 | | | | | | |
| | MBIR | | | | | | |
| Low-dose protocol 3 | FBP | 80 | 15 | 0.5 | 0.99 ^a | 25.11 ^a | 0.1 |
| | ASIR-50 | | | | 0.82 ^b | 23.08 ^b | |
| | ASIR-100 | | | | | | |
| | MBIR | | | | | | |
| Low-dose protocol 4 | FBP | 80 | 10 | 0.5 | 0.53 ^a | 13.38 ^a | 0.1 |
| | ASIR-50 | | | | 0.44 ^b | 12.29 ^b | |
| | ASIR-100 | | | | | | |
| | MBIR | | | | | | |

^a Cadaver 1^b Cadaver 2^c Calculated by CTEXPO software

exposures. In addition to the FBP standard reconstruction, all images were reconstructed using the following IRTs: ASIR-50, ASIR-100, and MBIR. The ASIR percentage could be selected in a spectrum of 0–100%, where ASIR-50 meant 50% FBP and 50% ASIR, and ASIR-100 meant 100% ASIR. Bone convolution kernel was used in the images of cadaver 1 (except MBIR for which only standard convolution kernel was available). A standard reconstruction kernel was used in all the images of cadaver 2. The CTDIvol and dose length product (DLP) were obtained from the digital imaging and communication in medicine (DICOM) tags. In addition, effective doses were calculated using CT-Expo version 2.1 (Medical University Hannover, Germany), an MS Excel application for assessing the radiation doses delivered to patients undergoing CT examinations based on the scan parameters of the used scanner type. The tissue weighting factors used were those from the International Commission on Radiologic Protection Document ICRP 103 [22]. A protocol summary is shown in Table 1.

Processing and viewing of 3D datasets

Each of the 40 MDCT datasets was converted to DICOM format and uploaded onto a shared Google Drive. The DICOM

datasets were then imported into a 3D image reformatting software (OnDemand Software, version 1.0, Cybermed Inc., Seoul, South Korea). The images were viewed on a 22" flat panel LCD color monitor in landscape mode (Dell P2210, Round Rock, Texas, USA). Specifications of the monitor were as follows: aspect ratio: 16:10; screen resolution 1680 × 1050 (highest, recommended) (calculated pixel size: 0.282 mm); color resolution: 32 bit; luminance 250 Cd/m²; contrast ratio (static): 1000:1. The window width/level of the MDCT images was set to 3000/650, and the images were viewed and measurements recorded in a dimly lit room.

Sample selection

The maxillary and mandibular edentulous ridges of both the imaged cadavers provided the study sample sites. The sample site inclusion criteria were all edentulous spaces within the jaws of the cadavers, at 5-mm intervals. The exclusion criteria for the edentulous spaces were the following: the presence of foreign objects or artificial defects at the residual ridge, and areas of residual ridges with bucco-lingual or occluso-apical dimensions of less than 2 mm.

Based on the inclusion criteria, the posterior regions of the jaws of cadaver 1 and the entire jaws of cadaver 2 were

Table 2 Distribution of sample sites

| Cadaver | Maxillary sites | | Mandibular sites | | Total |
|---------------------------------|-----------------|-------|------------------|-------|-------|
| | Premolar | Molar | Premolar | Molar | |
| 1 (bone convolution kernel) | 4 | 7 | 5 | 13 | 29 |
| 2 (standard convolution kernel) | 0 | 0 | 0 | 19 | 19 |
| Total | 4 | 7 | 5 | 32 | 48 |

considered for inclusion in the study. The entire maxilla of cadaver 2 and the two posterior-most sites from the left maxilla of cadaver 1 were excluded because the bucco-lingual or occluso-apical dimensions were less than 2mm. And the anterior mandible of cadaver 2 was excluded because of the presence of foreign objects or artificial defects.

A total of 48 sample sites were obtained, and two measurements, the ridge height and width, were obtained from each site, yielding 96 sample measurements from each protocol. Table 2 displays the distribution of the sample sites. Each of the 48 sample sites was examined in all the MDCT protocols (1 reference and 19 test protocols) for a total of 960 sites examined, and 1920 measurements.

Reformatting of sample sites

One oral and maxillofacial radiologist (A.A.) with 10 years of experience in CT image processing and analysis performed the reformatting of all the datasets to obtain transverse cross-sectional images of the sample sites. The 3D module of the OnDemand software was used to produce each cross section individually. The text overlay information was turned off in order to mask the mA and kVp. Since the cadaver heads were not moved between the MDCT examinations, the default position and orientation of the orthogonal sectional planes relative to the jaws were consistent in all the MDCT datasets of each cadaver. Thus, standardization of the site and orientation of the reformatted sample sites was achievable through measured shift and angulation of the orthogonal sectional planes. Tables 3 and 4 show sample sites obtained with each of the 20 combinations of exposure protocols and reconstruction techniques using a bone kernel and standard kernel, respectively. Each reformatted site was saved as a bookmark on the master database of the reformatting software (on the hard drive of the computer) such that the examiners can access the reformatted sites using the OnDemand software.

Recording the test measurements

The examiners, two oral and maxillofacial radiologists (R.A. and R.S.) with 14 and 8 years of experience, respectively, in CT image processing and analysis, recorded the test measurements using the Ruler tool of the software. The examiners

were blinded to all exposure parameters and reconstruction protocols.

The height measurement of the ridge was recorded on the sample site along the line representing the oblique sagittal plane, and the width measurement along the line representing the axial plane (Fig. 1). The limits of the height and width measurements were the outer cortical boundaries of the bone (Fig. 2). The linear measurements were recorded to the nearest 0.1 mm. The examiners were calibrated in identification of the outer margin of the bony ridges and were permitted to adjust magnification of the images for optimum clarity, but not the window width and level.

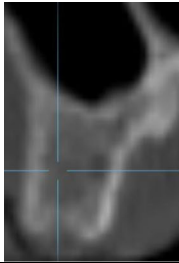
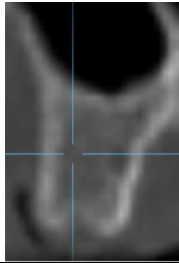
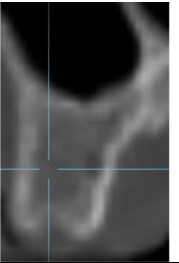
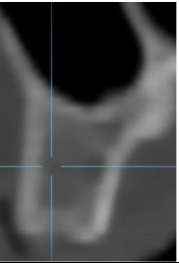
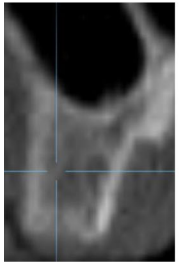
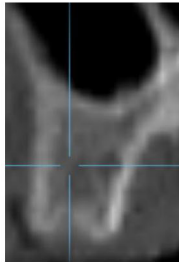
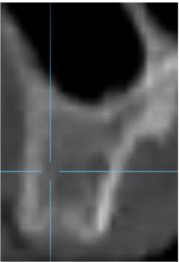
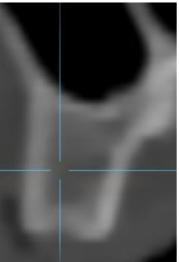
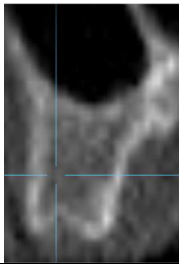
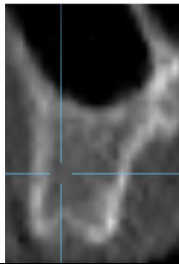
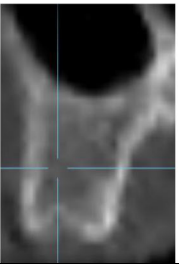
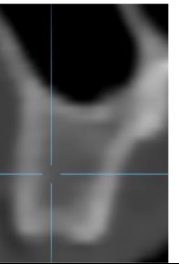
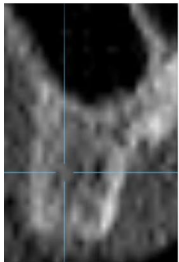
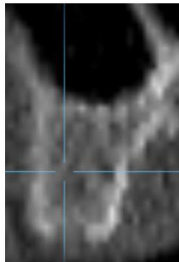
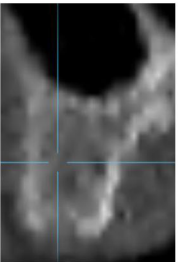
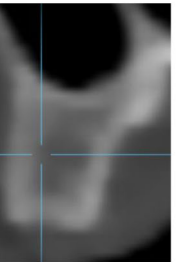
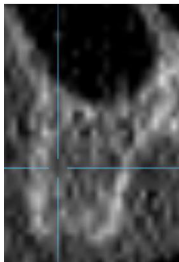
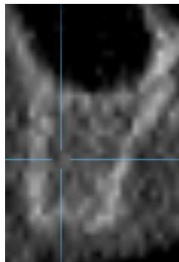
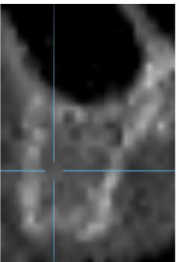
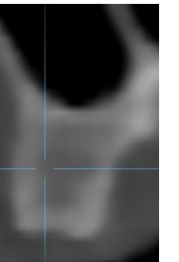
One examiner (R.S.) recorded all the measurements once (1920 measurements from 960 sites). Then 100 sample sites were selected for testing intra- and inter-examiner reliability. The sites were equally distributed among the imaging protocols. Five samples were selected from each imaging protocol: Three samples were randomly selected from cadaver 1 and two samples were randomly selected from cadaver 2. Random selection was performed using an online random number generator (<http://stattrek.com/statistics/random-number-generator.aspx>). Each examiner, independently, recorded the height and width measurements from the 100 sites. Thus, 200 measurements were obtained to calculate the intra- and inter-examiner reliability.

Statistical analysis

The recorded measurements were analyzed with the statistical program SPSS, version 22 (IBM, Armonk, New York, USA). The intra- and inter-examiner reliability were both calculated by two statistical tests (for confirmation of the results): Cronbach's alpha and inter-item Correlation.

Descriptive statistics were used to analyze the differences in the linear measurements between the reference protocol (reference dose with FBP) and each of the other imaging protocols. Agreement between the linear measurements was determined with Bland–Altman plots (produced with SPSS, version 22). Linear regression was used to test for proportional bias; if a significant variance of differences was found across the range of mean values, a logarithmic transformation of the differences was applied and the statistical analysis repeated [23]. Statistical significance was set at a *P*-value of 0.05.

Table 3 Images of a sample site obtained with the various combinations of exposure protocols and reconstruction techniques using a bone convolution kernel (except MBIR which used a standard convolution kernel)

| | Filtered Backprojection | ASIR 50 | ASIR 100 | MBIR |
|-------------------------|---|--|---|---|
| Reference dose protocol |  |  |  |  |
| Low dose protocol 1 |  |  |  |  |
| Low dose protocol 2 |  |  |  |  |
| Low dose protocol 3 |  |  |  |  |
| Low dose protocol 4 |  |  |  |  |

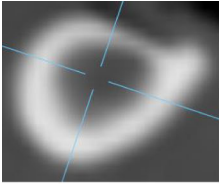
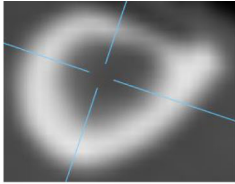
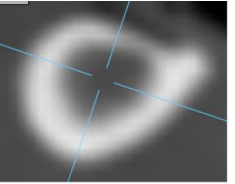
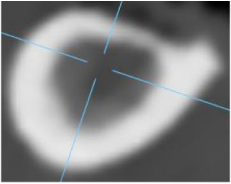
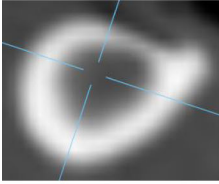
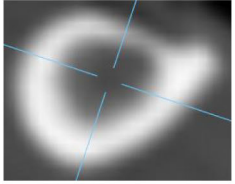
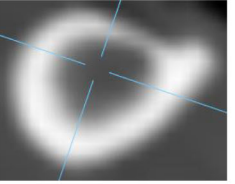

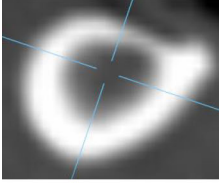
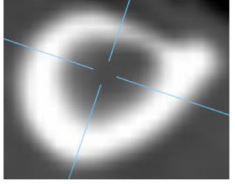
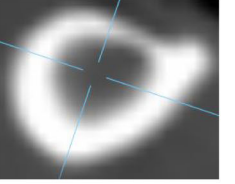
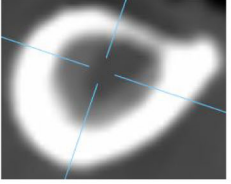
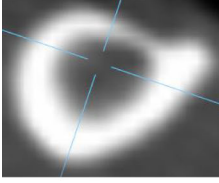
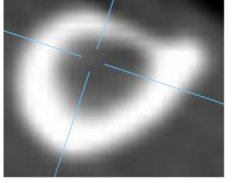
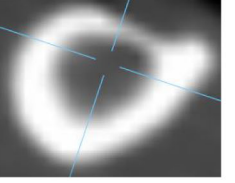


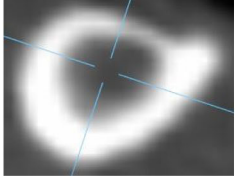


Vertical and horizontal lines within the images demonstrate the standardized position and orientation of the measurement lines

Results

Both the intra- and inter-examiner reliability scores for the linear ridge dimensions demonstrated very high reli-

ability. The Cronbach’s alpha and inter-item correlation scores for the intra-examiner reliability were both 0.999 and, for the inter-examiner reliability, were 0.996 and 0.992, respectively.

Table 4 Images of a sample site obtained with the various combinations of exposure protocols and reconstruction techniques using a standard convolution kernel

| | Filtered Backprojection | ASIR 50 | ASIR 100 | MBIR |
|-------------------------|---|---|--|---|
| Reference dose protocol |  |  |  |  |
| Low dose protocol 1 |  |  |  |  |
| Low dose protocol 2 |  |  |  |  |
| Low dose protocol 3 |  |  |  |  |
| Low dose protocol 4 |  |  |  |  |

Vertical and horizontal lines within the images demonstrate the standardized position and orientation of the measurement lines

Using a bone kernel, images became grainier with progressive dose reduction, with the graininess more marked with FBP, followed by ASIR-50 and then ASIR-100 (Table 3). With a standard kernel, no visible graininess was detected with the naked eye (Table 4). Despite the variable image quality, Bland–Altman plots (Online Resources 1 and 2) with linear regression showed no systematic variation between the linear measurements obtained with the reference protocol and the other imaging protocols (Table 5). The only exceptions were LD 3/ASIR-50 (bone kernel) and LD 4/ASIR-100 (bone and standard kernels). The mean measurement dif-

ferences between these three protocols and the reference protocol were within ± 0.1 mm, with the 95% confidence interval limits being within the range of ± 1.15 mm.

Discussion

The present study attempts to contribute to the dose optimization for MDCT in dental implant site imaging through investigating the validity of linear measurements of ridge dimensions using 19 different test combinations of dose protocols and reconstruction techniques. The linear mea-

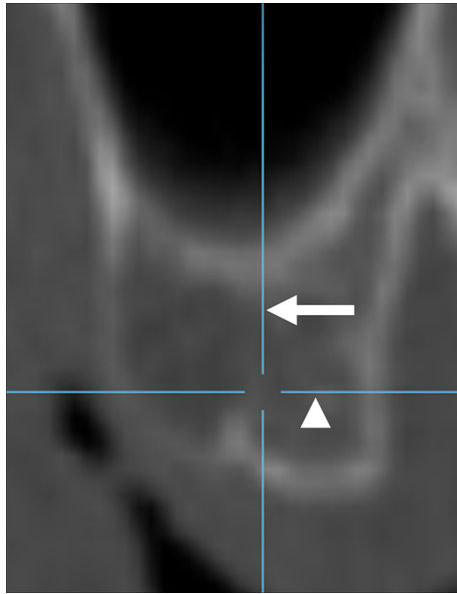


Fig. 1 Sample site from the posterior maxilla (obtained using the reference-dose protocol and filtered backprojection) showing position and orientation of linear measurements: the height measurement along the line representing the oblique sagittal plane (*arrow*) and the width measurement along the *line* representing the axial plane (*arrowhead*)

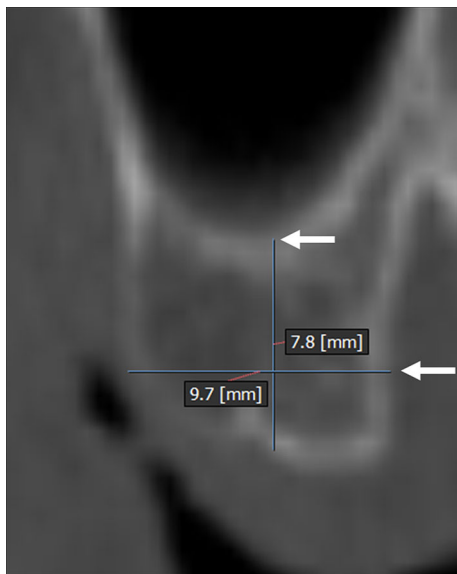


Fig. 2 Sample site from the posterior maxilla (obtained using the reference-dose protocol and filtered backprojection) showing the limits of the height and width measurements at the outer cortical boundaries of the ridge (*arrows*)

measurements obtained with most of the test protocols were comparable to those from the reference protocol. For those protocols which demonstrated statistically significant differences in linear measurements, the differences were small, being similar to the differences reported between reference-dose FBP protocols and the gold standard of direct bone

measurements [7]. However, in order to determine which dose/reconstruction technique yields the highest accuracy, comparison of the measurements obtained with the ultralow-dose protocols with direct bone measurements is needed.

The high intra- and inter-examiner reliability measures obtained in the present study are in agreement with other studies which recorded ridge dimensions from MDCT images of the jaws [8,24]. Watanabe et al. [24] obtained correlation values for intra-observer variability and inter-observer agreement of 0.99 and 0.97, respectively, and Suomalainen et al. [8] reported that the intra-class correlations between the intra- and inter-observer readings obtained in their study showed almost perfect matches.

The comparable linear measurements were obtained despite variable degrees of graininess seen in the images obtained with the different imaging protocols. The variable degrees of graininess seen in the present study with the different imaging protocols are compatible with the findings of Widmann et al. [13], who have reported that MBIR has proven to be the most powerful method for noise reduction and allowed 93 % noise reduction as compared with 30 % using ASIR-50 and 56 % using ASIR-100, and with the findings of another study by the authors (under review) which found a significant difference in objective noise measurements between the reconstruction techniques when a bone kernel was used. The variable degrees of graininess seen in the present study are also compatible with the results of Widmann et al. (2016) who found variable contrast-to-noise ratios with dose/reconstruction technique combinations similar to those used in the present study [25]. Thus, the types of IRT tested in the present study and the percentage of statistical iterations in ASIR, although yielding images with different levels of graininess, had no significant impact on the recorded linear measurements when compared to FBP.

The comparable measurements obtained in the present study with the reference-dose and low-dose FBP protocols are in agreement with the findings of Hara et al. [26], who found that ASIR was comparable with FBP, in terms of spatial resolution, when comparing high-contrast objects. The findings are also comparable to those of Widmann et al. [27] who found that the use of low-dose MDCT protocols with similar scan parameters and FBP had no influence on target registration errors in computer-assisted surgery, and are also compatible with the findings of Suomalainen et al. [4] who found that an approximately 80 % reduction in dose with FBP did not alter the modulation transfer function of two MDCT devices, despite markedly reduced CNR.

The high-contrast nature of the diagnostic task being investigated in the present study is one of the factors which may have aided in adequate identification of the bony margins, even at very low doses with FBP. For recording the linear dimensions of edentulous ridges requires identification of the bone–soft tissue interface which is a task that may

Table 5 Differences between the linear measurements obtained by the reference protocol (reference dose/filtered backprojection) and the various imaging protocols using bone and standard convolution kernels (except MBIR with which a standard kernel only was used) (LD: low-dose protocol)

| | Bone kernel | | | | | Standard kernel | | | | |
|-------------------|----------------------|--|--------------------------------------|-------------|--------------------------|----------------------|--|--------------------------------------|-------------|--------------------------|
| | Mean difference (mm) | Standard deviation of the differences (mm) | 95 % Confidence interval limits (mm) | | Sig. (linear regression) | Mean difference (mm) | Standard deviation of the differences (mm) | 95 % Confidence interval limits (mm) | | Sig. (linear regression) |
| | | | Upper limit | Lower limit | | | | Upper limit | Lower limit | |
| Ref dose/ASIR-50 | -0.0328 | 0.4620 | 0.8728 | -0.9384 | 0.986 | -0.0737 | 0.2617 | 0.4392 | -0.5866 | 0.489 |
| Ref dose/ASIR-100 | 0.2310 | 0.4489 | 1.1108 | -0.6488 | 0.061 | 0.0105 | 0.2729 | 0.5454 | -0.5244 | 0.535 |
| Ref dose/MBIR | -0.0174 | 0.4927 | 0.9482 | -0.9830 | 0.341 | 0.4305 | 0.3339 | 1.0851 | -0.2240 | 0.698 |
| LD 1/FBP | -0.1379 | 0.3820 | 0.6108 | -0.8866 | 0.287* | -0.1974 | 0.3123 | 0.4148 | -0.8096 | 0.860 |
| LD 1/ASIR-50 | 0.0328 | 0.3311 | 0.6817 | -0.6161 | 0.059 | 0.0368 | 0.3242 | 0.6722 | -0.5986 | 0.524 |
| LD 1/ASIR-100 | 0.2310 | 0.4489 | 1.1108 | -0.6488 | 0.053* | 0.0105 | 0.2729 | 0.5454 | -0.5244 | 0.638 |
| LD 1/MBIR | -0.0929 | 0.3958 | 0.6829 | -0.8687 | 0.465 | 0.3718 | 0.7580 | 1.8575 | -1.1138 | 0.604 |
| LD 2/FBP | 0.0724 | 0.4902 | 1.0332 | -0.8884 | 0.100 | -0.1553 | 0.3011 | 0.4348 | -0.7454 | 0.343 |
| LD 2/ASIR-50 | -0.0552 | 0.4558 | 0.8382 | -0.9486 | 0.746 | -0.1053 | 0.2681 | 0.4202 | -0.6307 | 0.140 |
| LD 2/ASIR-100 | -0.2195 | 0.4195 | 0.6028 | -1.0418 | 0.173 | -0.1342 | 0.3139 | 0.4810 | -0.7494 | 0.892 |
| LD 2/MBIR | 0.0262 | 0.5044 | 1.0148 | -0.9624 | 0.154 | 0.3863 | 0.2966 | 0.9677 | -0.1950 | 0.856 |
| LD 3/FBP | -0.1483 | 0.4342 | 0.7027 | -0.9993 | 0.607 | 0.0579 | 0.2919 | 0.6300 | -0.5142 | 0.234 |
| LD 3/ASIR-50 | 0.0655 | 0.5424 | 1.1287 | -0.9977 | 0.041* ^a | -0.0632 | 0.3291 | 0.5820 | -0.7083 | 0.471 |
| LD 3/ASIR-100 | -0.0224 | 0.4569 | 0.8732 | -0.9180 | 0.083 | 0.0974 | 0.3590 | 0.8011 | -0.6064 | 0.294 |
| LD 3/MBIR | -0.1162 | 0.5312 | 0.9249 | -1.1573 | 0.149 | 0.2284 | 0.2266 | 0.6726 | -0.2157 | 0.494 |
| LD 4/FBP | 0.0017 | 0.7266 | 1.4258 | -1.4224 | 0.125 | -0.0632 | 0.3737 | 0.6694 | -0.7957 | 0.179 |
| LD 4/ASIR-50 | -0.1362 | 0.5476 | 0.9372 | -1.2096 | 0.749 | -0.0789 | 0.7623 | 1.4152 | -1.5731 | 0.364 |
| LD 4/ASIR-100 | -0.0276 | 0.5712 | 1.0919 | -1.1471 | 0.008* ^a | 0.1000 | 0.2950 | 0.6782 | -0.4782 | 0.013* ^a |
| LD 4/MBIR | -0.1998 | 0.5204 | 0.8202 | -1.2198 | 0.684 | 0.2903 | 0.3197 | 0.9169 | -0.3364 | 0.619 |

* After logarithmic conversion

^a Significant at $p = 0.05$

tolerate the level of noise seen in low-dose FBP examinations. The low pitch used in the present study is another possible reason for the comparable results between the low-dose and standard-dose protocols. Maintaining a low pitch factor may have allowed faithful reproduction of the bony margins, with no loss of information through interpolation (which occurs at unacceptably high pitch factors) [28]. As such, at the doses tested and with the high-contrast diagnostic task tested, ASIR and MBIR did not provide an advantage over FBP.

The reference protocol used in the present study is similar to the standard protocols used for implant site imaging [29]. The test protocols in the present study utilized progressively decreasing mAs settings with variable kV, with the effective dose imparted by the lowest dose protocols estimated at being 2.5% of the reference dose. The estimated effective doses achieved in the present study are markedly less than those reported by Suomalainen et al. [4], despite the fact that the present study's CT examinations included wider scan lengths including the entire skull and mandible. It should be noted, however, that the wide scan length used in the present study is not usually used when imaging the jaws for implant site assessment. The wide scan length was used because the images were also utilized for other studies which were not limited to the jaws. Thus, if the present study's test protocols are used for limited imaging of one or both jaws, they are expected to impart markedly lower effective doses than those estimated for the present study.

When comparing the dose reductions achieved by various studies, it may be misleading to compare their reported effective doses only, since the effective dose is directly influenced by the scan length, which may be variable between studies. The CTDIvol may be a better parameter for comparison of dose reductions between MDCT devices and protocols since it measures the amount of radiation delivered to a particular scan volume for a standardized phantom taking into account scan pitch [30]. When the lowest CTDIvol achieved in the present study was compared to the lowest CTDIvol reported by three studies which demonstrated acceptable linear measurement accuracy of dental implant sites, the present study's CTDIvol was found to be 78% lower [8, 10, 11]. Although the present study utilized a lower pitch value than that used by Loubele et al. [10], a lower CTDIvol was achieved in the present study because the mAs was lower. Our results, therefore, support considerably reducing the mAs for dose reduction.

It must be noted, however, that cone beam CT (CBCT) has become a very popular technique for dental implant site evaluation and has been advocated as imparting lower doses than MDCT. As such, comparison of the radiation doses imparted by ultralow-dose MDCT protocols and CBCT is warranted. However, CBCT shows a wide range in doses, overlapping with those from MDCT and panoramic radiography, depending on field of view, imaging parameters and manufacturer

[31–33]. Kyriakou et al. [34] calculated the CTDIw of four different CBCT scanners, which ranged between 2.3 and 3.1 mGy. The lowest dose levels of the MDCT protocols tested in the present study were well below these values. In addition, the calculated effective doses imparted by the ultralow-dose MDCT protocols in the present study are also lower than those reported for many dentomaxillofacial CBCT devices [32]. Furthermore, as mentioned above, the use of shorter MDCT scan lengths than those used in the present study is expected to impart even lower MDCT doses with the ultralow-dose protocols.

One of the limitations of the present study, however, is that most of the sample sites were at the mandibular molar region. The thick cortication of the bone in this region may have made it easier to detect the bone–soft tissue boundaries compared to the boundaries at other areas of the jaws (maxilla and anterior regions of both jaws). The bone–soft tissue interface at the posterior mandible is also easier to identify than the roof of the inferior alveolar canal (IAC), which requires both higher contrast and spatial resolution. Another limitation is that the test measurements were not compared to a true gold standard. For measurement accuracy is best assessed when compared to physical measurements recorded directly from the bone.

Therefore, further studies are recommended to investigate the effect of more aggressive dose reductions in combination with ASIR and MBIR through raising the pitch factor coupled with the lowest possible mAs. The use of bone convolution kernels with MBIR to possibly overcome smoothing effects may also be investigated. Dose optimization using IRTs may also be tested for the increasingly popular use of computer-aided implant surgery. Studying the accuracy of measurements recorded from ultralow-dose protocols as compared to direct physical measurements from cadavers is also recommended, with such studies including sample sites from all areas of the jaws, as well as accuracy of detection of the roof of the IAC [35]. And future studies may also be limited to one or both jaws in order to allow more meaningful estimates of effective doses.

Conclusions

A nearly 97.5% reduction in dose did not significantly affect the height and width measurements of edentulous jaws regardless of the reconstruction algorithm used, which may benefit high accuracy-dependent tasks such as active computer-aided implant surgery. More aggressive dose reductions and additional diagnostic tasks should be investigated using ASIR and MBIR.

Acknowledgments The authors wish to thank the individuals who donated their bodies and tissues for the advancement of education and research, and Ms. Eidah Alenazi, MSc (Assistant Researcher, Statistics

& Operations Research Department, King Saud University), for kindly providing statistical advice for this manuscript.

Compliance with ethical standards

Conflict of interest The authors declare that they have no conflict of interest.

Ethical standard All procedures performed in studies involving human participants were in accordance with the ethical standards of the institutional and/or national research committee and with the 1964 Declaration of Helsinki and its later amendments or comparable ethical standards. Informed consent was obtained from all individual participants included in the study.

References

- United Nations Scientific Committee on the Effects of Atomic Radiation Sources and Effects of Ionizing Radiation (2010) In: Official Records of the General Assembly, Sixty-third Session, Supplement No. 46., New York, (2010) 2008. United Nations
- Loubele M, Bogaerts R, Van Dijck E, Pauwels R, Vanheusden S, Suetens P, Marchal G, Sanderink G, Jacobs R (2009) Comparison between effective radiation dose of CBCT and MSCT scanners for dentomaxillofacial applications. *Eur J Radiol* 71(3):461–468
- Ludlow JB, Ivanovic M (2008) Comparative dosimetry of dental CBCT devices and 64-slice CT for oral and maxillofacial radiology. *Oral Surg Oral Med Oral Pathol Oral Radiol Endod* 106(1):106–114. doi:10.1016/j.tripleo.2008.03.018
- Suomalainen A, Kiljunen T, Kaser Y, Peltola J, Kortensniemi M (2009) Dosimetry and image quality of four dental cone beam computed tomography scanners compared with multislice computed tomography scanners. *Dentomaxillofac Radiol* 38(6):367–378. doi:10.1259/dmfr/15779208
- Kalra MK, Maher MM, Toth TL, Hamberg LM, Blake MA, Shepard JA, Saini S (2004) Strategies for CT radiation dose optimization. *Radiology* 230(3):619–628. doi:10.1148/radiol.2303021726
- Tyndall DA, Price JB, Tetradis S, Ganz SD, Hildebolt C, Scarfe WC (2012) Position statement of the American Academy of Oral and Maxillofacial Radiology on selection criteria for the use of radiology in dental implantology with emphasis on cone beam computed tomography. *Oral Surg Oral Med Oral Pathol Oral Radiol* 113(6):817–826
- Al-Ekrish A, Ekram M (2011) A comparative study of the accuracy and reliability of multidetector computed tomography and cone beam computed tomography in the assessment of dental implant site dimensions. *Dentomaxillofac Radiol* 40(2):67–75
- Suomalainen A, Vehmas T, Kortensniemi M, Robinson S, Peltola J (2008) Accuracy of linear measurements using dental cone beam and conventional multislice computed tomography. *Dentomaxillofac Radiol* 37(1):10–17. doi:10.1259/dmfr/14140281
- Rustemeyer P, Streubüher U, Suttmoeller J (2004) Low-dose dental computed tomography: significant dose reduction without loss of image quality. *Acta Radiol* 45:847–853
- Loubele M, Jacobs R, Maes F, Schutyser F, Debaveye D, Bogaerts R, Coudyzer W, Vandermeulen D, Van Cleynenbreugel J, Marchal G (2005) Radiation dose vs. image quality for low-dose CT protocols of the head for maxillofacial surgery and oral implant planning. *Radiat Protect Dosim* 117(1–3):211–216
- Rustemeyer P, Streubüher U, Suttmoeller J (2004) Low-dose dental computed tomography: significant dose reduction without loss of image quality. *Acta Radiol* 45(8):847–853
- Silva AC, Lawder HJ, Hara A, Kujak J, Pavlicek W (2010) Innovations in CT dose reduction strategy: application of the adaptive statistical iterative reconstruction algorithm. *Am J Roentgenol* 194(1):191–199. doi:10.2214/ajr.09.2953
- Widmann G, Dalla Torre D, Hoermann R, Schullian P, Gassner EM, Bale R, Puelacher W (2015) Ultralow-dose computed tomography imaging for surgery of midfacial and orbital fractures using ASIR and MBIR. *Int J Oral Maxillofac Surg* 44(4):441–446. doi:10.1016/j.ijom.2015.01.011
- McCullough CH, Leng S, Sunnegardh J, Vrieze TJ, Yu L, Lane J, Raupach R, Stierstorfer K, Flohr T (2013) Spatial resolution improvement and dose reduction potential for inner ear CT imaging using a z-axis deconvolution technique. *Med Phys* 40(6):061904. doi:10.1118/1.4802730
- Niu YT, Mehta D, Zhang ZR, Zhang YX, Liu YF, Kang TL, Xian JF, Wang ZC (2012) Radiation dose reduction in temporal bone CT with iterative reconstruction technique. *AJNR Am J Neuroradiol* 33(6):1020–1026. doi:10.3174/ajnr.A2941
- Schulz B, Beeres M, Bodelle B, Bauer R, Al-Butmeh F, Thahammer A, Vogl TJ, Kerl JM (2013) Performance of iterative image reconstruction in CT of the paranasal sinuses: a phantom study. *AJNR Am J Neuroradiol* 34(5):1072–1076. doi:10.3174/ajnr.A3339
- Widmann G, Schullian P, Gassner E-M, Hoermann R, Bale R, Puelacher W (2015) Ultralow-dose CT of the craniofacial bone for navigated surgery using adaptive statistical iterative reconstruction and model-based iterative reconstruction: 2D and 3D image quality. *Am J Roentgenol* 204(3):563–569
- McCullough CH, Chen GH, Kalender W, Leng S, Samei E, Taguchi K, Wang G, Yu L, Pettigrew RI (2012) Achieving routine submillisievert CT scanning: report from the summit on management of radiation dose in CT. *Radiology* 264(2):567–580
- McHanwell S, Brenner E, Chirulescu A, Drukker J, van Mameren H, Mazzotti G, Pais D, Paulsen F, Plaisant O, Caillaud M, Laforêt E, Riederer B, Sanudo J, Bueno-Lopez J, Donate F, Sprumont P, Teofilovski-Parapid G, Moxham B (2008) The legal and ethical framework governing body donation in Europe—a review of current practice and recommendations for good practice. *Eur J Anat* 12(1):1–24
- Riederer B, Bolt S, Brenner E, Bueno-Lopez J, Cirulescu A, Davies D, De Caro R, Gerrits P, McHanwell S, Pais D, Paulsen F, Plaisant O, Sendemir E, Stabile I, Moxham B (2012) The legal and ethical framework governing body donation in Europe—1st update on current practice. *Eur J Anat* 16(1):1–21
- Platzer W, Putz R, Poisel S (1978) Ein neues Konservierungs- und Aufbewahrungssystem für anatomisches Material. *Acta Anat (Basel)* 102(1):60–67
- ICRP (2007) The 2007 Recommendations of the International Commission on Radiological Protection. ICRP Publication 103. *Ann ICRP* 37:2–4
- Bland JM, Altman D (1986) Statistical methods for assessing agreement between two methods of clinical measurement. *Lancet* 327(8476):307–310
- Watanabe H, Abdul MM, Kurabayashi T, Aoki H (2010) Mandible size and morphology determined with CT on a premise of dental implant operation. *Surg Radiol Anat* 32(4):343–349
- Widmann G, Bischel A, Stratis A, Kakar A, Bosmans H, Jacobs R, Gassner E-M, Puelacher W, Pauwels R (2016) Ultralow dose dentomaxillofacial CT imaging and iterative reconstruction techniques: variability of Hounsfield Units and contrast-to-noise ratio. *Br J Radiol* 89(1060):20151055. doi:10.1259/bjr.20151055
- Hara AK, Paden RG, Silva AC, Kujak JL, Lawder HJ, Pavlicek W (2009) Iterative reconstruction technique for reducing body radiation dose at CT: feasibility study. *Am J Roentgenol* 193(3):764–771
- Widmann G, Fasser M, Schullian P, Zangerl A, Puelacher W, Kral F, Riechelmann H, Jaschke W, Bale R (2012) Substantial

- dose reduction in modern multi-slice spiral computed tomography (MSCT)-guided craniofacial and skull base surgery. *RoFo. Fortschritte auf dem Gebiete der Rontgenstrahlen und der Nuklearmedizin* 184(2):136–142
28. Goldman LW (2008) Principles of CT: multislice CT. *J Nucl Med Technol* 36(2):57–68. doi:[10.2967/jnmt.107.044826](https://doi.org/10.2967/jnmt.107.044826)
 29. GE Medical Systems (2010) Advantage Dentascan operator manual 2182400-100. vol revision 4. General Electric Company
 30. McCollough CH, Primak AN, Braun N, Kofler J, Yu L, Christner J (2009) Strategies for reducing radiation dose in CT. *Radiol Clin N Am* 47(1):27–40. doi:[10.1016/j.rcl.2008.10.006](https://doi.org/10.1016/j.rcl.2008.10.006)
 31. Bornstein MM, Scarfe WC, Vaughn VM, Jacobs R (2014) Cone beam computed tomography in implant dentistry: a systematic review focusing on guidelines, indications, and radiation dose risks. *Int J Oral Maxillofac Implants* 29(Suppl):55–77
 32. Ludlow J, Timothy R, Walker C, Hunter R, Benavides E, Samuelson D, Scheske M (2015) Effective dose of dental CBCT—a meta analysis of published data and additional data for nine CBCT units. *Dento Maxillofac Radiol* 44(1):20140197
 33. Pauwels R (2015) Cone beam CT for dental and maxillofacial imaging: dose matters. *Radiat Prot Dosim* 165(1–4):156–161. doi:[10.1093/rpd/ncv057](https://doi.org/10.1093/rpd/ncv057)
 34. Kyriakou Y, Kolditz D, Langner O, Krause J, Kalender W (2011) Digital volume tomography (DVT) and multislice spiral CT (MSCT): an objective examination of dose and image quality. *Rofo* 183(2):144–153. doi:[10.1055/s-0029-1245709](https://doi.org/10.1055/s-0029-1245709)
 35. Vercruyssen M, Fortin T, Widmann G, Jacobs R, Quirynen M (2014) Different techniques of static/dynamic guided implant surgery: modalities and indications. *Periodontol* 2000 66(1):214–227